nation $\mathbf{k}''-\mathbf{k}$. This allows us to sum (A6) first over $\mathbf{k}$, keeping $\mathbf{k}''-\mathbf{k}$ fixed, which leads to

$$\delta\Psi=\sum_{\mathbf{k}',\mathbf{k}''-\mathbf{k},\sigma',e,f} J(e,f;\mathbf{k}''-\mathbf{k},\mathbf{k}') \times(\epsilon_{\mathbf{k}'+\mathbf{k}-\mathbf{k}''}{}^{e}-\epsilon_{\mathbf{k}'}{}^{f})^{-1}\exp[i(\mathbf{k}''-\mathbf{k})\cdot\mathbf{R}] \times c_{\mathbf{k}'+(\mathbf{k}-\mathbf{k}''),\sigma}{}^{e*}c_{\mathbf{k}',\sigma'}{}^{f}c^{d*}(\mathbf{R},\sigma')\Psi_0. \quad \text{(A8)}$$

This is the expression used in the text, which is entirely analogous to the polarization accompanying nuclear indirect exchange. Clearly there are also both the nonlocalized parts and terms in which, instead of $c^{d*}(\mathbf{r},\sigma')$, we have excitations into empty bands e'. We expect that smaller exchange integrals J, and increasing energy denominators, will make these effects quite negligible.

PHYSICAL REVIEW VOLUME 115, NUMBER 1 JULY 1, 1959

Antiferromagnetic Structures of MnS_2, $MnSe_2$, and $MnTe_2$†

J. M. HASTINGS, N. ELLIOTT, AND L. M. CORLISS
Chemistry Department, Brookhaven National Laboratory, Upton, New York

(Received February 13, 1959)

The antiferromagnetic structures of MnS_2, $MnSe_2$, and $MnTe_2$ have been obtained by neutron diffraction. The disulfide exhibits ordering of the "third" kind, the ditelluride, ordering of the "first" kind, and the diselenide, an arrangement which is intermediate between the two. The structures are discussed from the viewpoint of indirect exchange. Magnetic susceptibilities, obtained by the Gouy method, are reported for all three compounds.

NEUTRON diffraction studies of the three polymorphic forms of MnS have shown[1] that the antiferromagnetic structures developed in these materials may be correlated with crystal structure. More specifically, in α-MnS, second nearest neighbor manganese atoms are joined by sulfur atoms located on octahedral sites, whereas in the two β forms, tetrahedrally coordinated sulfur atoms join nearest neighbor manganese atoms. Furthermore, the separation and spatial arrangement of manganese atoms are the same in both α-MnS and the zinc blende form of MnS. The observed magnetic structures indicate that strong antiferromagnetic correlations exist between second nearest neighbors in the case of α-MnS and between nearest neighbors in the two β forms. Indirect exchange coupling thus appears to involve octahedral sulfur bonds in the first instance and tetrahedral bonds in the second.

In an effort to further elucidate the role of the anion in antiferromagnetism, these studies have been extended to the homologous series consisting of MnS_2, $MnSe_2$, and $MnTe_2$. These compounds crystallize with the pyrite structure, which is a NaCl-like arrangement of M and X_2 groups with the axes of the X_2 groups parallel to the various body diagonals. The structure is shown schematically in Fig. 1. A salient feature is the presence of nearly regular tetrahedra whose corner positions are occupied by three metal atoms and one member of an X_2 group, and whose center is occupied by the other member of the X_2 pair. Magnetic as well as crystal-chemical evidence[2] suggest that these compounds may be regarded as essentially ionic combinations of Mn^{+2} and $X_2^{=}$ groups. From this point of view, the face-centered cubic structure of manganese ions might be expected to exhibit second nearest neighbor antiferromagnetic correlations as in MnO and α-MnS. On the other hand, the existence of nearly tetrahedral Mn-X-Mn linkages between nearest neighbor manganese atoms would suggest the possibility of an ordering scheme based upon nearest neighbor antiferromagnetic correlations as in β-MnS. It would not appear possible at present to predict, either on theoretical grounds or on the basis of empirical knowledge of antiferromagnetic

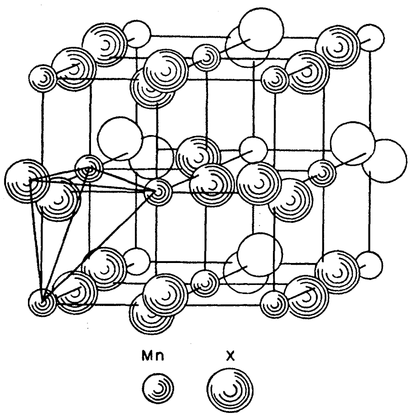

FIG. 1. The pyrite structure.

[†] Research performed under the auspices of the U. S. Atomic Energy Commission. A preliminary account of this work has been published in J. Appl. Phys. **29**, 391 (1958).

[1] Corliss, Elliott, and Hastings, Phys. Rev. **104**, 924 (1956).

[2] N. Elliott, J. Am. Chem. Soc. **59**, 1958 (1937); L. Néel and R. Benoit, Compt. rend. **237**, 444 (1953).

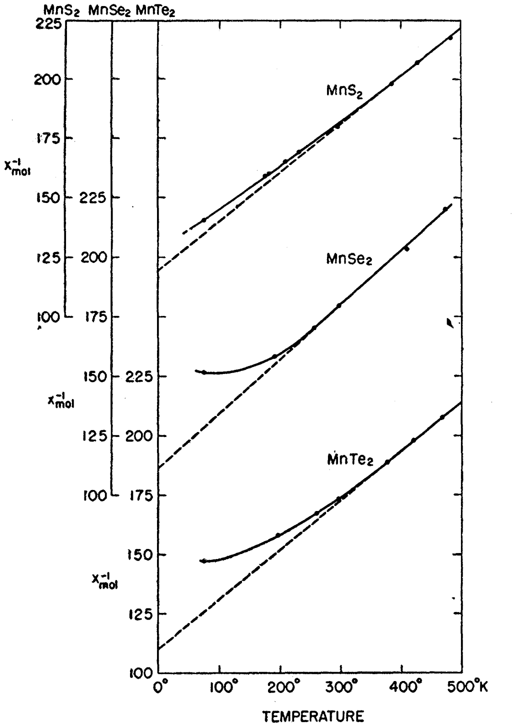

FIG. 2. Inverse susceptibilities of MnS$_2$, MnSe$_2$, and MnTe$_2$ as a function of temperature.

structures, which, if any, of these magnetic structures the manganese pyrites would exhibit.

SAMPLE PREPARATION AND SUSCEPTIBILITY MEASUREMENTS

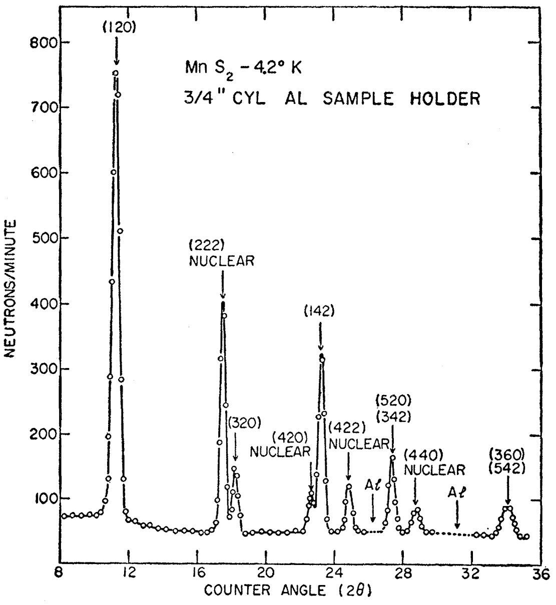

FIG. 3. Neutron diffraction pattern of MnS$_2$.

TABLE I. Molar magnetic susceptibilities of MnS$_2$, MnSe$_2$, and MnTe$_2$.

MnS$_2$		MnSe$_2$		MnTe$_2$	
T°K	$\chi_{mole}\times10^6$	T°K	$\chi_{mole}\times10^6$	T°K	$\chi_{mole}\times10^6$
76	7150	76	6600	76	6800
177	6310	193	6330	197	6350
183	6250	258	5880	262	5990
210	6065	300	5565	297	5780
233	5925	411	4900	378	5305
296	5550	475	4545	423	5050
386	5060			470	4820
418	4820				
483	4580				

Specimens of MnSe$_2$ and MnTe$_2$ were prepared by direct synthesis from the elements.[2] Crystals of very pure hauerite from Raddusa, Sicily, were obtained through the Ward's Natural Science Establishment, Incorporated, Rochester, New York.

The magnetic susceptibilities of several samples of each compound were measured by the Gouy method in the temperature range 76°–500°K. The results, uncorrected for diamagnetism, are given in Table I. Assuming a Curie-Weiss law at the higher temperatures, values of θ and μ_{eff} were calculated and are tabulated in Table II. The data are also shown graphically in Fig. 2.

NEUTRON DIFFRACTION DATA AND THE ASSIGNMENT OF ANTIFERROMAGNETIC STRUCTURES

Neutron diffraction patterns for the three compounds taken at 4.2°K and a wavelength of 1.064 A are shown in Figs. 3, 4, and 5. In addition, patterns were obtained at room temperature, which is well above the Néel point in all three cases. In all three low-temperature patterns, magnetic superstructure peaks are clearly developed and indicate the occurrence of three different antiferromagnetic structures. There are several peaks in which magnetic superstructure reflections are superimposed on nuclear fundamental reflections. These mixed peaks arise because the fundamental nuclear contributions to them are due only to the anion and hence the magnetic superstructure lines, coming solely from the manganese, can occur at the same positions. The magnetic contributions to the mixed peaks were obtained by subtracting the room temperature pattern with the appropriate Debye-Waller correction.

The pyrite space group, $Pa3$, places the manganese in positions 4(a) and the X_2 group in positions 8(c) with one parameter, u. The u parameter was determined from the room-temperature diffraction patterns and is given in Table III for the three compounds. In addition, the table lists the Mn-X and X-X distances as well as the Mn-X-Mn angle. In the course of this phase of the

TABLE II. Curie-Weiss constants obtained from susceptibility data.

	MnS$_2$	MnSe$_2$	MnTe$_2$
θ(°K)	592°	483°	528°
μ_{eff}	6.30β	5.93β	6.22β

TABLE III. Structural data obtained from room-temperature diffraction data.

Compound	a_0	u parameter X-rays[a,b]	u parameter Neutrons	Mn−X distance	X−X distance[c]	Mn−X−Mn angle[c]
MnS_2	6.097 A	0.4012 ± 0.0004	0.4040 ± 0.0005	2.60 A	2.03 ± 0.01 A	112.1°
$MnSe_2$	6.417 A	0.393 ± 0.001	0.3954 ± 0.0008	2.71 A	2.33 ± 0.02 A	113.8°
$MnTe_2$	6.943 A	0.386 ± 0.002	0.386 ± 0.001	2.90 A	2.74 ± 0.03 A	115.4°

[a] N. Elliott, J. Am. Chem. Soc. **59**, 1958 (1937).
[b] F. Offner, Z. Krist. **89**, 182 (1934).
[c] Based on neutron value for u parameter.

structure determination, the coherent scattering amplitude of Te was redetermined. From a diffraction pattern of PbTe, having the rock-salt structure, the amplitude of Te was obtained relative to that of Pb. Using a value of 0.957×10^{-12} cm for the scattering amplitude of Pb, the scattering amplitude of Te is computed to be $(0.59 \pm 0.01) \times 10^{-12}$ cm, a value slightly higher, but agreeing within the combined limits of error, with the value $(0.56 \pm 0.02) \times 10^{-12}$ cm given in the most recent tabulation of cross sections.[3]

The magnetic scattering pattern for MnS_2 can be indexed on a cubic cell whose edge is twice that of the chemical cell. The observed magnetic reflections follow the indicial rule: $h = 2n+1$, $k = 2n$, $l = 2n$, $h \neq k \neq l$. This rule identifies the magnetic structure as ordering of the third kind shown in Fig. 6. The spin direction is parallel to the unique axis, i.e., the axis along which the spins alternate. A comparison of observed and calculated intensities using this model and a moment for Mn^{+2} corresponding to five unpaired electrons is given in Table IV.

The magnetic diffraction pattern for $MnTe_2$ can be indexed using the original chemical unit cell, with $h = 2n$, $k = 2n$, $l = 2n+1$ and $h = 2n+1$, $k = 2n+1$, $l = 2n$. This implies that the magnetic structure is an ordering of the first kind which is shown in Fig. 6. The spin direction required to obtain a satisfactory fit, places the spins in the ferromagnetic sheets. The orientation within the sheet cannot be determined, in this case, from powder data. On the basis of this model and using five unpaired electrons in computing the manganese moment, excellent agreement is obtained between the calculated and observed intensities listed in Table V.

The third compound, $MnSe_2$, requires a tripling of the original chemical unit cell along one axis in order to index the diffraction pattern. The observed magnetic peaks are ones for which $h+k = 2n+1$ and $k+l = 2n+1$, where h corresponds to the elongated axis. The structure which accounts for these peaks is shown in Fig. 6. If one chooses a spin direction parallel to the long axis of the cell, a fit is obtained between calculated and observed intensities as shown in Table VI. Once again, the manganese moment was assumed to correspond to five unpaired electrons.

In computing the integrated intensities, the previously established form factor for Mn^{+2} [1] was used. A composite of the previous data as well as the present ones is shown in Fig. 7. The curve in the figure was computed from Hartree's latest calculation for Mn^{+2}

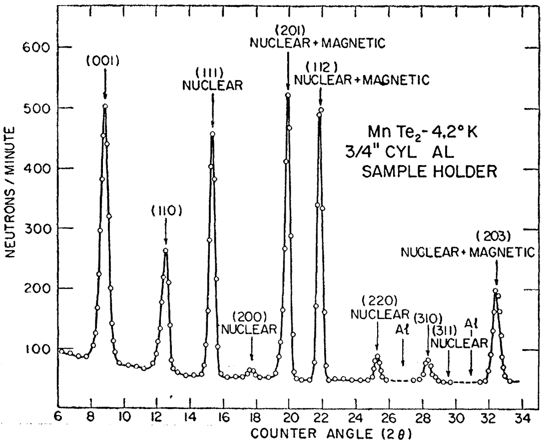

FIG. 4. Neutron diffraction pattern of $MnTe_2$.

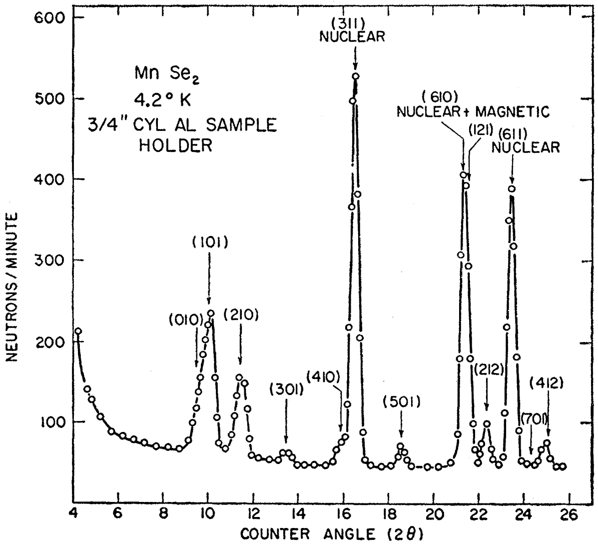

FIG. 5. Neutron diffraction pattern of $MnSe_2$.

---

[3] *Neutron Cross Sections*, compiled by D. J. Hughes and R. Schwartz, Brookhaven National Laboratory Report BNL-325 (Superintendent of Documents, U. S. Government Printing Office, Washington, D. C., 1958), second edition.

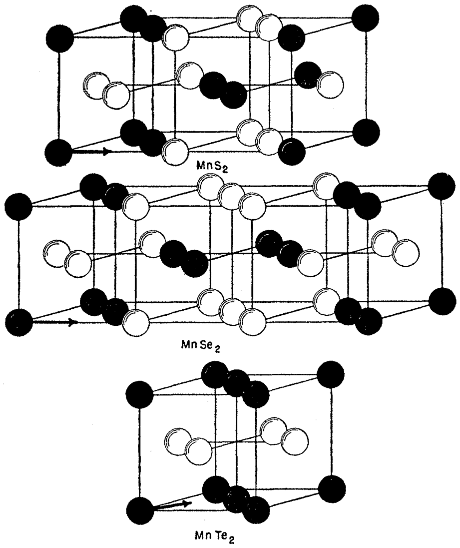

FIG. 6. Magnetic structure of MnS_2 (ordering of the "third" kind), $MnSe_2$, and $MnTe_2$ (ordering of the "first" kind). Positive and negative orientations of the dipoles are shown by black and white spheres. The direction of the magnetic axis relative to the crystallographic axes is shown by an arrow. In the case of $MnTe_2$ the spin direction lies in the ferromagnetic sheets, but orientation within the plane is unspecified.

including exchange.[4] In order to obtain a fit with the experimental points, the abscissa for the computed form factor curve was scaled by a factor of 0.9. This is equivalent to assigning a mean radius for the *d*-shell distribution of the Mn^{+2} ions in these compounds which is ten percent greater than the free-ion value.

DISCUSSION

The compounds MnO, α-MnS, and MnSe, all crystallizing with the rock salt structure, possess a single antiferromagnetic structure in common. In the case of the series MnS_2, $MnSe_2$, and $MnTe_2$, considerably more variety is encountered. The magnetic moment configurations are different in all three compounds and the magnetic unit cell size varies as well, being equal to the chemical cell in the case of $MnTe_2$, twice the chemical cell in the case of MnS_2, and three times the chemical cell in the case of $MnSe_2$. Despite these differences, the three antiferromagnetic structures are similar in certain significant respects. This can best be seen by considering the distribution of parallel and antiparallel neighbors. In all three compounds the Mn atoms have eight nearest neighbors with antiparallel spin and four nearest neighbors with parallel spin. This is the maximum antiferromagnetic nearest neighbor correlation that can be uniformly propagated in the face-centered cubic structure and corresponds to the arrangement observed in the zinc blende form of MnS. This strongly suggests that the Mn-X-Mn tetrahedral linkage provides the important path for indirect exchange.

TABLE IV. Calculated and observed integrated intensities for magnetic peaks of MnS_2.

hkl	Calculated intensities	Observed intensities
120	3783	3643
320	414	420
142	1193	1195
520, 342	528	537
542, 360	212	228

The differences in the various antiferromagnetic structures manifest themselves in the second nearest neighbor arrangements. In the case of the ditelluride (ordering of the first kind) all six second nearest neighbors are parallel to the central atom. In the disulfide (ordering of the third kind) each Mn atom has four parallel and two antiparallel second nearest neighbors. In the case of the diselenide, which does not develop a homogeneously ordered structure, two-thirds of the Mn atoms have five parallel and one antiparallel second nearest neighbors and one-third of the Mn atoms have four parallel and two antiparallel second nearest neighbors. Thus in all cases the second nearest neighbor interaction is ferromagnetic, with the number of ferromagnetic interactions increasing in the order MnS_2, $MnSe_2$, $MnTe_2$.

A convenient short-hand description for the three structures can be developed in terms of the way in which successive planes are related. In Fig. 6 the horizontal direction in the plane of the paper is taken to be the x-axis. If we denote by A and B the first two y-z planes at the left and by $\bar{A}$ and $\bar{B}$ the same planes with magnetic moment directions reversed, then the three structures can be represented by the following repeat sequences:

$$MnS_2\text{:}\quad A\,B\,\bar{A}\,\bar{B}\,A\,\cdots,$$
$$MnSe_2\text{:}\quad A\,B\,\bar{A}\,\bar{B}\,\bar{A}\,B\,A\,\cdots,$$
$$MnTe_2\text{:}\quad \mathrm{A\,B\,A}\,\cdots.$$

Actually, the B planes are identical with the A planes except for a glide parallel to the y-axis of one-half the cell edge. The $\bar{A}$ plane can be obtained from the A plane

TABLE V. Calculated and observed integrated intensities for the magnetic peaks of $MnTe_2$.

hkl	Calculated intensities	Observed intensities
001	4147	4115
110	1854	1866
201	1248	1227
112	1291	1096
310	284	335
203	286	265

---

[4] D. R. Hartree, *The Calculation of Atomic Structures* (John Wiley & Sons, Inc., New York, 1957).

TABLE VI. Calculated and observed integrated intensities for the magnetic peaks of $MnSe_2$.

hkl	Calculated intensities	Observed intensities
010	347	2675
101	2205	
210	1241	1349
301	149	142
410	278	Unresolved
501	132	124
610	16	Unresolved
121	608	Unresolved
212	514	462
701	32	30
412	281	266

either by reversal of signs or by a diagonal glide in the y-z plane of length equal to one-half the face diagonal. From this point of view the complex $MnSe_2$ structure can be thought of as being composed of units of the $MnTe_2$ structure in which either a sign reversal or diagonal glide has taken place between units. It is interesting to note that the sequence of planes in the structure corresponding to ordering of the second kind (MnO, α-MnS) is exactly the same as in the case of ordering of the third kind. The difference between the two structures arises solely from the difference in configuration within the A plane.

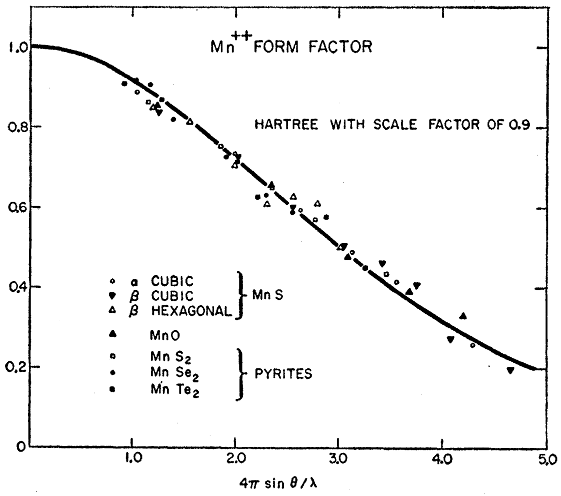

FIG. 7. Composite magnetic form factor for Mn^{+2}. The solid curve represents the form factor computed from Hartree's calculation for Mn^{+2}, including exchange, and adjusted as explained in the text.

Keffer and O'Sullivan[5] have computed the magnetic dipolar energy for arrays of spins corresponding to ordering of the third kind. They find that the energy is a minimum when all dipoles point parallel to the direction in which the unit cell is enlarged (the x-direction of Fig. 6). Furthermore, they point out that this result is in disagreement with the moment direction obtained for the zinc blende form of MnS from neutron diffraction data, which place the dipoles at right angles to the x-axis. In MnS_2, as the present work shows, the spin direction is parallel to the x-axis, in agreement with the predictions of Keffer and O'Sullivan. However, the two results taken together indicate that the agreement may be fortuitous and that there are indeed important contributions to the anisotropy which have not been considered in the calculations.

---

[5] F. Keffer and W. O'Sullivan, Phys. Rev. **108**, 637 (1957). T. Nagamiya, Osaka University, Japan (private communication) confirms these calculations for ordering of the third kind.